

# Helicons in multi-Weyl semimetals

Shiv Kumar Ram

*Department of Physics, Lalit Narayan Mithila University, Darbhanga, Bihar 846004, India*

Amit Gupta

*Department of Physics, M. R. M. College, Lalit Narayan Mithila University, Darbhanga, Bihar 846004, India*

(Dated: April 23, 2025)

Helicons are transverse electromagnetic modes in three dimension(3D) electron systems in the presence of a static magnetic field. This modes have been proposed in isotropic or single Weyl semimetals(sWSMs) (Francesco M.D. Pellegrino et al, Phys. Rev. B **92**, 201407(R) (2015)). In this work, we extend our study to investigate helicons modes in gapless multi-Weyl semimetals(mWSMs) within semiclassical Boltzmann approach and discuss the differences that arise compared to single Weyl semimetals.

## I. INTRODUCTION

Helicons are low-frequency, circularly polarized transverse electromagnetic waves propagating in a three dimensional(3D) conducting medium under a static magnetic field ( $\mathbf{B}$ ) [1–3]. In conventional metals/plasmas, they follow a quadratic dispersion relation [4]

$$\omega = \frac{k^2 B}{\mu_0 n_e e} \quad (1)$$

where  $n_e$  is electron density and  $k$  is wave vector. Helicons couple strongly to plasmons (collective charge oscillations), leading to helicon-plasmon polaritons: new hybrid modes with tunable frequencies and anomalous absorption peaks in optical conductivity.

Weyl semimetal is a three-dimensional topological state of matter, in which the conduction and valence bands touch at a finite number of nodes, called Weyl nodes[5–10]. Each Weyl node can be regarded as a monopole in  $k$ -space carrying the topological charge  $n=1$ . Weyl semimetal has the Fermi arc surface states that connect the surface projections of two Weyl nodes [3]. Weyl semimetals introduce an axion term  $\theta(\mathbf{E} \cdot \mathbf{B})$  in Maxwell's equations due to their topological magnetoelectric effect, altering helicon dispersion [11]

$$\omega \sim \frac{k^2 B}{\mu_0 n_e e} + k \quad (2)$$

The second term originates due to the topological  $\theta$  term. This work has been studied for isotropic or single WSMS with the inclusion of orbital magnetic moment(OMM) [11]. The OMM can be thought as self-rotation of the Bloch wave packet, and modify the energy of the Bloch electron under the external magnetic field [12]. bital moment  $m_s(\mathbf{k})$  and anisotropic contributions to the distribution function. Helicons in Weyl semimetals are a rich testbed for topological electrodynamics, blending condensed matter physics with electromagnetic wave theory. Their unique properties—governed by chiral anomaly, Berry curvature, and axion fields—enable

novel device concepts while posing intriguing theoretical challenges. Helicon modes in Weyl semimetals are modified due to pseudofields (e.g., strain-induced gauge fields) refines pseudohelicons [13].

In this paper, we extend our corresponding study to the case of multi-WSMs (higher topological charge larger than one). The multi-WSMs can be think of merger of multiple Weyl points of same chirality results anisotropic dispersion relations in  $\mathbf{k}$  space [7, 8, 14]. Multi-WSMs show some intriguing transport phenomena [15–22]. We observe the helicon modes in multi-WSMs(topological charge  $J=2,3$ ) have the same linear and quadratic dispersion relations as in the case of isotropic WSM(topological charge  $J=1$ ) but they are renormalized by corresponding plasma frequency  $\omega_{p,J}$ . We also obtain expression for cyclotron frequency  $\omega_{cJ}$  up to quadratic powers of magnetic field  $B$ .

## II. MODEL HAMILTONIAN AND SEMICLASSICAL BOLTZMANN APPROACH

The modification of the Maxwell's equations due to the axion term  $\theta(\mathbf{r}, t) = 2(\mathbf{b} \cdot \mathbf{r} - b_0 t)$ , where  $\mathbf{b}(\mathbf{b}_0)$  denotes separation of nodes in momentum(energy) space [11, 23]

$$\mathcal{L} = \frac{1}{8\pi}(E^2 - B^2) - \rho\varphi + \mathbf{J} \cdot \mathbf{A} + \mathcal{L}_\theta \quad (3)$$

where

$$\mathcal{L}_\theta = -\frac{\alpha}{4\pi^2}\theta(\mathbf{r}, t)\mathbf{E} \cdot \mathbf{B} \quad (4)$$

where  $\alpha = e/(\hbar c) \approx 1/327$  is the usual fine-structure constant and  $\theta(\mathbf{r}, t) = 2(\mathbf{b} \cdot \mathbf{r} - b_0 t)$  is the axion angle. The axion term  $\theta(\mathbf{r}, t)$  modified two of the Maxwell's equations

$$\nabla \cdot \mathbf{D} = (\rho + \frac{\alpha}{2\pi^2}\mathbf{b} \cdot \mathbf{B}) \quad (5)$$

$$\nabla \cdot \mathbf{B} = 0 \quad (6)$$

$$\nabla \times \mathbf{E} = -\frac{1}{c} \frac{\partial \mathbf{B}}{\partial t} \quad (7)$$

$$-\frac{\partial \mathbf{D}}{\partial t} + \nabla \times \mathbf{B} = \frac{4\pi}{c} (\mathbf{J} - \frac{\alpha}{2\pi^2} \mathbf{b} \times \mathbf{E} + \frac{\alpha}{2\pi^2} b_0 \mathbf{B}) \quad (8)$$

Accordingly, wave equation for the electric field propagation is modified to be

$$-\epsilon_b \frac{\partial^2 \mathbf{E}}{\partial t^2} - \nabla \times \nabla \times \mathbf{E} = \frac{\partial \mathbf{J}}{\partial t} - \frac{\alpha}{\pi} \mathbf{b} \times \frac{\partial \mathbf{E}}{\partial t} - \frac{\alpha}{\pi} b_0 \nabla \times \mathbf{E} \quad (9)$$

In the vicinity of a nodal point with chirality  $\chi$  and Berry monopole charge of magnitude  $J$ , the low-energy effective continuum Hamiltonian is given by [24–26]

$$\mathcal{H}(\mathbf{k}) = \mathbf{d}_s(\mathbf{k}) \cdot \boldsymbol{\sigma}, \quad (10)$$

with  $k_\perp = \sqrt{k_x^2 + k_y^2}$  and  $\phi_k = \arctan(\frac{k_y}{k_x})$

$$\mathbf{d}_s(\mathbf{k}) = \{\alpha_J k_\perp^J \cos(J\phi_k), \alpha_J k_\perp^J \sin(J\phi_k), s v_F k_z\} \quad (11)$$

where  $\boldsymbol{\sigma} = \{\sigma_x, \sigma_y, \sigma_z\}$  the usual Pauli matrices,  $s \in \{1, -1\}$  denotes the chirality of the node, and  $v_F$  ( $v_\perp$ ) is the Fermi velocity along the  $z$ -direction ( $xy$ -plane). The eigenvalues of the Hamiltonian are given by

$$\epsilon_{\mathbf{k}} = \sqrt{\alpha_J^2 k_\perp^{2J} + v_z^2 k_z^2}, \quad (12)$$

where the value 1 (–1) for  $s$  represents the conduction (valence) band. We note that we recover the linear and isotropic nature of a WSM by setting  $J = 1$  and  $\alpha_1 = v_z$ . For a given chirality  $s = \pm$  of a single Weyl node, the semiclassical Boltzmann equation in equilibrium can be written as

$$\frac{\partial \tilde{f}^s}{\partial t} + \dot{\mathbf{k}} \cdot \frac{\partial \tilde{f}^s}{\partial \mathbf{k}} + \dot{\mathbf{r}} \cdot \frac{\partial \tilde{f}^s}{\partial \mathbf{r}} = 0 \quad (13)$$

Here,  $\tilde{f}^s$  is the electron distribution function.

In the presence of a static magnetic field  $\mathbf{B}$  and a time varying electric field  $\mathbf{E}$ , the semiclassical equations of motion are

$$\dot{\mathbf{r}} = \frac{1}{\hbar} \nabla_{\mathbf{K}} \tilde{\epsilon}_{\mathbf{k}}^s - \dot{\mathbf{k}} \times \boldsymbol{\Omega}_{\mathbf{k}}^s \quad (14)$$

$$\hbar \dot{\mathbf{k}} = -e\mathbf{E} - e\dot{\mathbf{r}} \times \mathbf{B} \quad (15)$$

where  $-e$  is the electron charge,  $\mathbf{E}$  and  $\mathbf{B}$  are external electric and magnetic fields, respectively.  $\boldsymbol{\Omega}_{\mathbf{k}}^s$  is the Berry curvature, and  $\tilde{\epsilon}_{\mathbf{k}}^s = \epsilon_{\mathbf{k}}^s - \mathbf{m}_{\mathbf{k}}^s \cdot \mathbf{B}$  with the orbital magnetic moment  $m_s(\mathbf{k})$  induced by the semiclassical “self-rotation” of the Bloch wave packet. The first term on the

right-hand side of Eq. (14) is  $\mathbf{v}_{\mathbf{k}}^s = \frac{1}{\hbar} \nabla_{\mathbf{k}} \tilde{\epsilon}_{\mathbf{k}}^s$ , defined in terms of an effective band dispersion  $\tilde{\epsilon}_s(\mathbf{k})$ . In topological metals such as WSMs, this quantity acquires a term due to the intrinsic orbital moment, i.e.,  $\tilde{\epsilon}_{\mathbf{k}}^s = \epsilon_{\mathbf{k}}^s - \mathbf{m}_{\mathbf{k}}^s \cdot \mathbf{B}$ , while  $\mathbf{m}_{\mathbf{k}}^s$  is the orbital moment induced by the semiclassical “self-rotation” of the Bloch wavepacket. The term  $\boldsymbol{\Omega}_{\mathbf{k}}^s$  is the Berry curvature [12, 27, 28]

$$\boldsymbol{\Omega}_{\mathbf{k}}^s = \text{Im}[\langle \nabla_{\mathbf{k}} u_{\mathbf{k}}^s | \times | \nabla_{\mathbf{k}} u_{\mathbf{k}}^s \rangle] \quad (16)$$

$$\mathbf{m}_{\mathbf{k}}^s = -\frac{e}{2\hbar} \text{Im}[\langle \nabla_{\mathbf{k}} u_{\mathbf{k}}^s | \times (\mathcal{H}_J(\mathbf{k}) - \epsilon_{\mathbf{k}}^s) | \nabla_{\mathbf{k}} u_{\mathbf{k}}^s \rangle] \quad (17)$$

where  $|u_{\mathbf{k}}^s\rangle$  satisfies the equation  $\mathcal{H}_J(\mathbf{k})|u_{\mathbf{k}}^s\rangle = \epsilon_{\mathbf{k}}^s|u_{\mathbf{k}}^s\rangle$

The general expressions for Berry curvature and orbital magnetic moment for multi-WSMs are [25]

$$\boldsymbol{\Omega}_{\mathbf{k}}^s = \pm \frac{s}{2} \frac{J v_F \alpha_J^2 k_\perp^{2J-2}}{\beta_{\mathbf{k},s}^3} \{k_x, k_y, Jk_z\} \quad (18)$$

$$\mathbf{m}_{\mathbf{k},s}^\pm = \frac{s}{2} \frac{e J v_F \alpha_J^2 k_\perp^{2J-2}}{\hbar \beta_{\mathbf{k},s}^2} \{k_x, k_y, Jk_z\} \quad (19)$$

where  $\beta_{\mathbf{k},s} = \sqrt{\alpha_J^2 k_\perp^{2J} + v_F^2 k_z^2}$  in the case of mWSMs.

From these expressions, we immediately observe the identity

$$\mathbf{m}_{\mathbf{k},s} = -e \epsilon_{\mathbf{k}} \boldsymbol{\Omega}_{\mathbf{k}}^s. \quad (20)$$

While the BC changes sign with  $s$ , the OMM does not.

By solving these coupled equations (14) and (15), one obtains

$$\dot{\mathbf{r}} = \frac{1}{\hbar D} \left[ \nabla_{\mathbf{k}} \tilde{\epsilon}_{\mathbf{k}} + e\mathbf{E} \times \boldsymbol{\Omega}_{\mathbf{k}}^s + \frac{e}{\hbar} (\nabla_{\mathbf{k}} \tilde{\epsilon}_{\mathbf{k}} \cdot \boldsymbol{\Omega}_{\mathbf{k}}^s) \mathbf{B} \right] \quad (21)$$

$$\dot{\mathbf{k}} = \frac{1}{\hbar D} \left[ -e\mathbf{E} - \nabla_{\mathbf{k}} \epsilon_{\mathbf{k}}^s \times \mathbf{B} - \frac{e^2}{\hbar} (\mathbf{E} \cdot \mathbf{B}) \boldsymbol{\Omega}_{\mathbf{k}}^s \right] \quad (22)$$

where the factor  $D = 1 + \frac{e}{\hbar} (\boldsymbol{\Omega}_{\mathbf{k}}^s \cdot \mathbf{B})$  modifies the phase space volume.

Equation (13) can be solved by expanding the distribution function in a linear power in the electric field as follows:

$$\tilde{f}^s = \tilde{f}_0^s + \tilde{f}_1^s e^{-i\omega t} \quad (23)$$

where  $\tilde{f}_1^s$  is linear in  $\mathbf{E}$  and is parametrized as follows

$$\tilde{f}_1^s = -\frac{\partial \tilde{f}_0^s}{\partial \epsilon_{\mathbf{k}}^s} (X_- e^{i\phi} + X_+ e^{-i\phi} + X_0) \quad (24)$$

The  $\tilde{f}_0^s(\epsilon_{\mathbf{k}}^s)$  can be expanded at low magnetic field as [11]

$$\begin{aligned}\tilde{f}_0^s(\tilde{\epsilon}_{\mathbf{k}}^s) &= \tilde{f}_0^s(\epsilon_{\mathbf{k}}^s - \mathbf{m}_{\mathbf{k}}^s \cdot \mathbf{B}) \\ &\simeq \tilde{f}_0^s(\epsilon_{\mathbf{k}}^s) - \mathbf{m}_{\mathbf{k}}^s \cdot \mathbf{B} \frac{\partial \tilde{f}_0^s(\epsilon_{\mathbf{k}}^s)}{\partial \epsilon_{\mathbf{k}}^s}\end{aligned}\quad (25)$$

From Eqs.(21) and Eq.(24), the expression for current density at time t is given by

$$\mathbf{j}_1 = -\frac{e}{(2\pi)^3} \int d^3k \left[ \tilde{\mathbf{v}}_{\mathbf{k}}^s + \frac{e}{\hbar} (\mathbf{\Omega}_{\mathbf{k}}^s \cdot \tilde{\mathbf{v}}_{\mathbf{k}}^s) \mathbf{B} \right] \tilde{f}_1^s \quad (26)$$

The above equation can be expressed in frequency space  $\omega$  as

$$j_a(\omega) = \sigma_{ab}(\omega) E_b(\omega) \quad (27)$$

In order to include the effects from the OMM and the BC, we first define the quantities

$$\tilde{\epsilon}_{\mathbf{k}}^s = \epsilon_{\mathbf{k}}^s - \mathbf{m}_{\mathbf{k}}^s \cdot \mathbf{B} \quad (28)$$

$$= \epsilon_{\mathbf{k}}^s + \epsilon_{\mathbf{k}}^{m,s} \quad (29)$$

with

$$\epsilon_{\mathbf{k}}^{m,s} = -\mathbf{B}_s \cdot \mathbf{m}_s(\mathbf{k})$$

The velocity in k-space is defined as

$$\mathbf{v}_s(\mathbf{k}) \equiv \nabla_{\mathbf{k}} \tilde{\epsilon}_{\mathbf{k}}^s = \mathbf{v}^{(0)}(\mathbf{k}) + \mathbf{v}_s^{(m)}(\mathbf{k}) \quad (30)$$

$$\mathbf{v}_s^{(m)}(\mathbf{k}) = \nabla_{\mathbf{k}} \epsilon_{\mathbf{k}}^{m,s} \quad (31)$$

where  $\epsilon_{\mathbf{k}}^{m,s}$  is the Zeeman-like correction to the energy due to the OMM,  $\mathbf{v}_s(\mathbf{k})$  is the modified band velocity of the Bloch electrons after including  $\epsilon_{\mathbf{k}}^{m,s}$ , and  $D$  is the modification factor of the phase space volume element due to a nonzero BC. Our weak-magnetic-field limit implies that

$$e |\mathbf{B} \cdot \mathbf{\Omega}_{\mathbf{k}}^s| \ll 1. \quad (32)$$

Inserting Eqs.(23) and (24) in Eq.(13), we find

$$X_{\pm} = \frac{e}{2D} \frac{k_{\perp} (E_x \pm iE_y)}{i[\omega \pm \frac{eBk_{\perp}}{D}]} \quad (33)$$

$$= \frac{e}{2D} \frac{k_{\perp} (E_x \pm iE_y)}{i[\omega \pm \omega_{c_J}]} \quad (34)$$

where  $\omega_{c_J} = \frac{eBk_{\perp}}{D}$  is the general expressions for cyclotron frequency of m-WSMs with J represents the topological charge. The expressions for cyclotron frequencies up to second order B are

$$\omega_{c_1} = Bev_F^2/\epsilon_F - sB^2e^2v_F^4 \cos \phi / (2\epsilon_F^3) \quad (35)$$

$$\omega_{c_2} = 2Be\alpha_2 \sin \phi + 4sB^2e^2\alpha_2^2 \cos^3 \phi / \epsilon_F \quad (36)$$

$$\begin{aligned}\omega_{c_3} &= 3Be\alpha_3^{2/3} \epsilon_F^{1/3} \sin^{4/3} \phi \\ &+ 9sB^2e^2\alpha_3^{4/3} \epsilon_F^{-1/3} \cos \phi (4 \cos^2 \phi + \sin \phi)\end{aligned} \quad (37)$$

with  $\epsilon_F$  represents the Fermi-energy of the multi-WSMs. and

$$X_0 = \frac{eE_z}{i\omega D} [v_{kz}^s + eB(\mathbf{\Omega}_{\mathbf{k}}^s \cdot \tilde{\mathbf{v}}_{\mathbf{k}}^s)] \quad (38)$$

Taking advantage of the azimuthal symmetry about the  $z$ -axis, we take advantage of the cylindrical coordinates defined by[26]

$$k_x = k_{\perp} \cos \phi, \quad k_y = k_{\perp} \sin \phi, \quad \text{and } k_z = k_z, \quad (39)$$

where  $k_{\perp} \in [0, \infty)$  and  $\phi \in [0, 2\pi)$ . We can rewrite velocity components(x and y) as

$$v_{k_x}^s = v_{k_{\perp}}^s \cos \phi, \quad v_{k_y}^s = v_{k_{\perp}}^s \sin \phi \quad (40)$$

with

$$\begin{aligned}v_{k_{\perp}}^s &= J \frac{\alpha_J^2 k_{\perp}^{2(J-1)+1}}{\epsilon(\mathbf{k})} \\ &+ seBJ^2 v_F \alpha_J^2 k_z k_{\perp}^{2(J-2)+1} \frac{(v_F^2 k_z^2 (J-1) - \alpha_J^2 k_{\perp}^{2J})}{\epsilon(\mathbf{k})^4}\end{aligned}\quad (41)$$

In the next step, we change variables from  $(k_{\perp}, k_z)$  to  $(\epsilon_{\mathbf{k}}, \varphi)$  by the coordinate transformation

$$k_{\perp} = \left( \frac{\epsilon_{\mathbf{k}}}{\alpha_J} \sin \varphi \right)^{1/J}, \quad k_z = \frac{\epsilon_{\mathbf{k}}}{v_F} \cos \varphi, \quad (43)$$

where  $\epsilon_{\mathbf{k}} \in [0, \infty)$  and  $\varphi \in [0, \pi)$ . The Jacobian of the transformation is  $\mathcal{J}(\epsilon_{\mathbf{k}}, \varphi) = \frac{1}{Jv_F \sin \varphi} \left( \frac{\epsilon_{\mathbf{k}} \sin \varphi}{\alpha_J} \right)^{1/J}$ , leading to analytical expressions for longitudinal conductivities  $\sigma_{zz}^J$  of multi-WSMs

$$\sigma_{zz}^1(\omega) = i \frac{e^2}{120\pi^2 v_F \omega \epsilon_F} (13B^2 e^2 v_F^4 + 20\epsilon_F^4) \quad (44)$$

$$\sigma_{zz}^2(\omega) = i \frac{e^2}{4\pi^2 \omega} \left( \frac{B^2 e^2 \pi v_F \alpha_2}{8\epsilon_F} + \frac{\pi v_F \epsilon_F}{4\alpha_2} \right) \quad (45)$$

and

$$\sigma_{zz}^3(\omega) = i \frac{e^2 v_F}{41496 \pi^{3/2} (\frac{\epsilon_F}{\alpha_3})^{2/3} \omega \Gamma(1/3)} \left( -\frac{81 B^2 e^2 (2\sqrt{3}\pi + 19\Gamma(1/3)\Gamma(2/3))}{\Gamma(7/6)} + \frac{1729 (\epsilon_F/\alpha_3)^{4/3} \Gamma(1/3)^2}{\Gamma(11/6)} \right) \quad (46)$$

The above components have been plotted in Fig.(1) for the parameters mentioned in caption of figure. The ana-

lytical expressions for transverse components of conductivities are not possible in low frequency limit.

$$\sigma_{xx}^{(2)}(\omega) = -\frac{e}{8\pi^2} \int_{-\infty}^{\infty} dk_z \int_0^{\infty} k_{\perp} dk_{\perp} \int_0^{\pi} d\phi \frac{e}{2D} v_{\perp}^2 \cos \phi^2 \left( \frac{1}{i[\omega + \frac{eBv_{\perp}}{Dk_{\perp}}]} + \frac{1}{i[\omega - \frac{eBv_{\perp}}{Dk_{\perp}}]} \right) \left( -\frac{\partial f_0^s}{\partial \epsilon_{\mathbf{k}}^s} \right) \quad (47)$$

$$\sigma_{xy}^{(2)}(\omega) = -\frac{e}{8\pi^2} \int_{-\infty}^{\infty} dk_z \int_0^{\infty} k_{\perp} dk_{\perp} \int_0^{\pi} d\phi \frac{e}{2D} v_{\perp}^2 \cos \phi^2 \left( \frac{1}{i[\omega + \frac{eBv_{\perp}}{Dk_{\perp}}]} - \frac{1}{i[\omega - \frac{eBv_{\perp}}{Dk_{\perp}}]} \right) \left( -\frac{\partial f_0^s}{\partial \epsilon_{\mathbf{k}}^s} \right) \quad (48)$$

We solve the above equations numerically up to quadratic powers in B and plotted in Fig(2) and Fig.(3). The leading power of B in Eq.(37) fix the values of cyclotron frequencies  $\omega_{c1}^0 = 5.68125 \times 10^{-5}$ ,  $\omega_{c2}^0 = 7.0902 \times 10^{-5} \sin \phi$ ,  $\omega_{c3}^0 = 3.49896 \times 10^{-4} \sin \phi^{4/3}$ . We can see that the leading part of cyclotron frequencies are decreasing with higher topological charges. These differences in the values of cyclotron frequencies distinguish the multi-WSMs.

Next, we define the dielectric tensor

$$\epsilon_{lm} = \delta_{lm} \epsilon_b + \frac{4\pi i}{\omega} \left[ \sigma_{lm} - \epsilon_{lmn} \frac{\alpha c}{2\pi^2} (b_n - q_n \frac{b_0}{\omega}) \right] \quad (49)$$

where  $\epsilon_{lmn}$  is Levi-Civita antisymmetric tensor and the indices l,m and n run over the cartesian coordinates x,y and z. The above equation can be combined with wave equation gives the following relation

$$\left( \frac{ck}{\omega} \right)^2 - \frac{2\alpha}{\pi c \omega} \left( b_z - \frac{b_0 k}{\omega} \right) = \epsilon_b + \frac{4\pi i}{\omega} (\sigma_{xx} - i\sigma_{xy}) \quad (50)$$

We can see that the transverse parts of the conductivities of multi-WSMs differ their dispersion relations. However, the linear and quadratic powers of k remains intact as in the case of single-WSMs [11]. The dispersion relations have been plotted in Fig.(4).

We will now calculate the gapped collective modes at  $\mathbf{B} = \mathbf{0}$ . In the long-wavelength limit, we find three gapped modes  $\Omega_{\lambda}(q)$  with  $\lambda = 1, 2, 3$  are given by

$$\Omega_{1,J}(k=0) = \omega_{-,J} \quad (51)$$

$$\Omega_{2,J}(k=0) = \omega_{p,J} / \sqrt{\epsilon_b} \quad (52)$$

$$\Omega_{3,J}(k=0) = \omega_{+,J} \quad (53)$$

where  $\omega_{\pm,J} = \alpha c b / (\pi \epsilon_b) \pm \sqrt{(\alpha c b)^2 / (\pi \epsilon_b)^2 + \omega_{p,J}^2 / \epsilon_b}$  with  $b = |\mathbf{b}|$

where  $\omega_{p,J}$  define the plasma frequencies in multi-WSMs.

$$\omega_{p,1}^2 = \frac{4e^2 \omega_{c1}^2}{3\pi \hbar v_F} \quad (54)$$

$$\omega_{p,2}^2 = \frac{\pi e^2 v_F}{4\alpha_2^2 \hbar} \quad (55)$$

$$\omega_{p,3}^2 = \frac{2\sqrt{\pi} e^2 v_F \omega^{2/3} \Gamma(1/3)}{9 \cdot 2^{2/3} \alpha_3^2 \hbar \Gamma(11/6)} \quad (56)$$

Therefore, the degeneracy of the three gapped collective modes at  $k=0$  is lifted by the presence of the axion term in the electromagnetic response of multi-WSMs. These modes can be distinguish by their corresponding plasma frequencies  $\omega_{p,J}$ .

### III. CONCLUSION

In summary, we have studied helicon modes in 3D multi-Weyl semimetal from semiclassical Boltzmann transport theory, with the inclusion of the axion term. We have calculated the analytical expressions for longitudinal part of conductivity tensor. The transverse parts of conductivity can be calculated numerically. The transverse components fix cyclotron frequencies in multi-WSMs and we have found that this frequency is lowest in triple-WSM and highest in single WSM. The degeneracy of the three gapped collective modes at  $k=0$  is lifted by the presence of the axion term in the electromagnetic response of multi-WSMs. These modes can be distinguish by their corresponding plasma frequencies  $\omega_{p,J}$ . Our work could distinguish the multi-WSMs with their differences in helicon modes in future experiments.

## IV. ACKNOWLEDGEMENTS

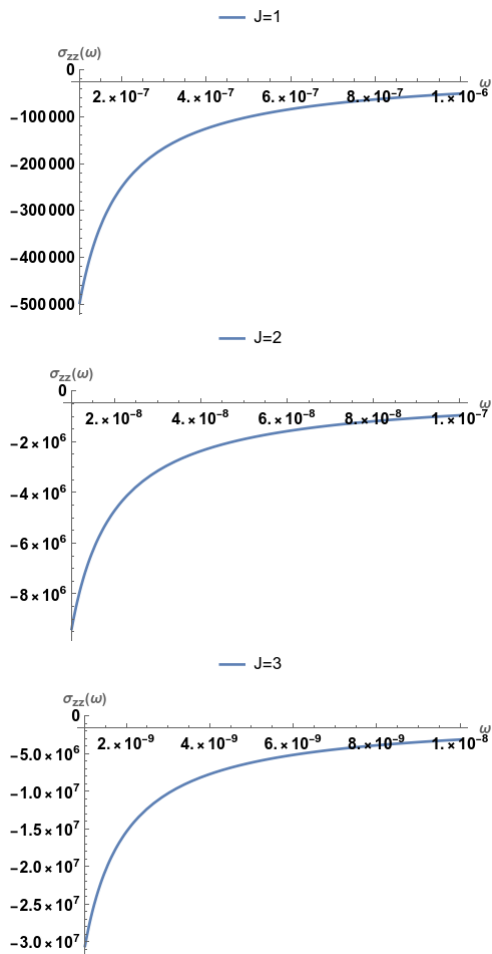


FIG. 1. The frequency dependence of the longitudinal optical conductivity at  $B = 3$ . The other parameters are taken as  $v_F = 0.005$ ,  $\mu = 0.4$ ,  $\alpha_2 = 3.9 \times 10^{-5}$  and  $\alpha_3 = 2.298 \times 10^{-6}$

We thank Debanand Sa for fruitful discussions.

- 
- [1] C. Kittel and P. McEuen, *Introduction to solid state physics* (John Wiley & Sons, 2018).
- [2] J. D. Jackson, *Classical electrodynamics* (John Wiley & Sons, 2021).
- [3] O. Konstantinov and V. Perel, Possible transmission of electromagnetic waves through a metal in a strong magnetic field, *SOVIET PHYSICS JETP-USSR* **11**, 117 (1960).
- [4] P. M. Platzman and P. A. Wolff, *Waves and interactions in solid state plasmas*, Vol. 13 (Academic Press New York, 1973).
- [5] X. Wan, A. M. Turner, A. Vishwanath, and S. Y. Savrasov, Topological semimetal and fermi-arc surface states in the electronic structure of pyrochlore iridates, *Physical Review B—Condensed Matter and Materials Physics* **83**, 205101 (2011).
- [6] A. Burkov and L. Balents, Weyl semimetal in a topological insulator multilayer, *Physical review letters* **107**, 127205 (2011).
- [7] G. Xu, H. Weng, Z. Wang, X. Dai, and Z. Fang, Chern semimetal and the quantized anomalous hall effect in hgr 2 se 4, *Physical review letters* **107**, 186806 (2011).
- [8] S.-M. Huang, S.-Y. Xu, I. Belopolski, C.-C. Lee, G. Chang, B. Wang, N. Alidoust, G. Bian, M. Neupane, C. Zhang, *et al.*, A weyl fermion semimetal with surface fermi arcs in the transition metal monopnictide taas class, *Nature communications* **6**, 7373 (2015).
- [9] B. Lv, N. Xu, H. Weng, J. Ma, P. Richard, X. Huang, L. Zhao, G. Chen, C. Matt, F. Bisti, *et al.*, Observation of weyl nodes in taas, *Nature Physics* **11**, 724 (2015).
- [10] S.-Y. Xu, I. Belopolski, N. Alidoust, M. Neupane, G. Bian, C. Zhang, R. Sankar, G. Chang, Z. Yuan, C.-C. Lee, *et al.*, Discovery of a weyl fermion semimetal and topological fermi arcs, *Science* **349**, 613 (2015).
- [11] F. M. Pellegrino, M. I. Katsnelson, and M. Polini, Helicons in weyl semimetals, *Physical Review B* **92**, 201407 (2015).
- [12] G. Sundaram and Q. Niu, Wave-packet dynamics in slowly perturbed crystals: Gradient corrections and

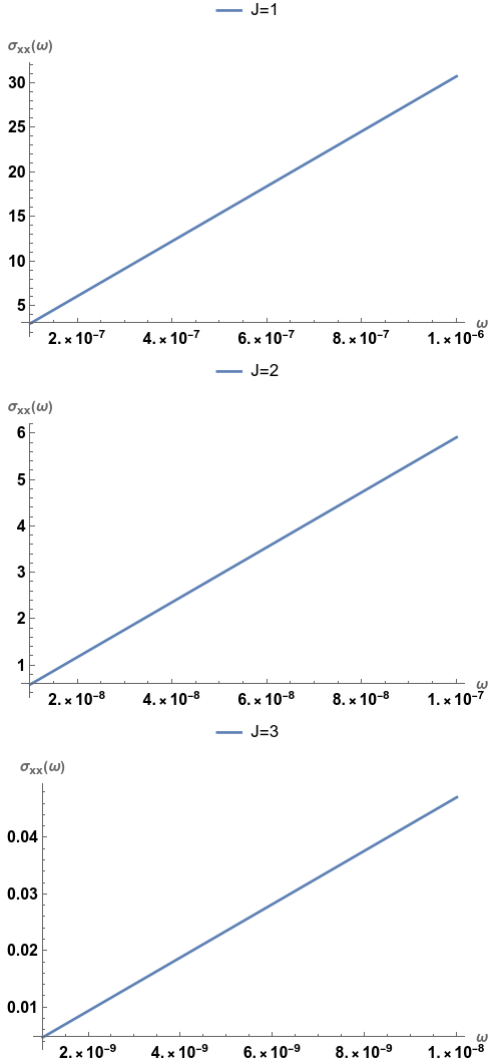


FIG. 2. The frequency dependence of the transverse optical conductivity at  $B = 3$ . The other parameters are taken as  $v_F = 0.005$ ,  $\mu = 0.4$ ,  $\alpha_2 = 3.9 \times 10^{-5}$  and  $\alpha_3 = 2.298 \times 10^{-6}$

- berry-phase effects, *Physical Review B* **59**, 14915 (1999).
- [13] E. Gorbar, V. Miransky, I. Shovkovy, and P. Sukhachov, Pseudomagnetic helicons, *Physical Review B* **95**, 115422 (2017).
- [14] S.-M. Huang, S.-Y. Xu, I. Belopolski, C.-C. Lee, G. Chang, T.-R. Chang, B. Wang, N. Alidoust, G. Bian, M. Neupane, *et al.*, New type of weyl semimetal with quadratic double weyl fermions, *Proceedings of the National Academy of Sciences* **113**, 1180 (2016).
- [15] S. Ahn, E. Mele, and H. Min, Optical conductivity of multi-weyl semimetals, *Physical Review B* **95**, 161112 (2017).
- [16] S. Mukherjee and J. Carbotte, Doping and tilting on optics in noncentrosymmetric multi-weyl semimetals, *Physical Review B* **97**, 045150 (2018).
- [17] T. Nag, A. Menon, and B. Basu, Thermoelectric transport properties of floquet multi-weyl semimetals, *Physical Review B* **102**, 014307 (2020).

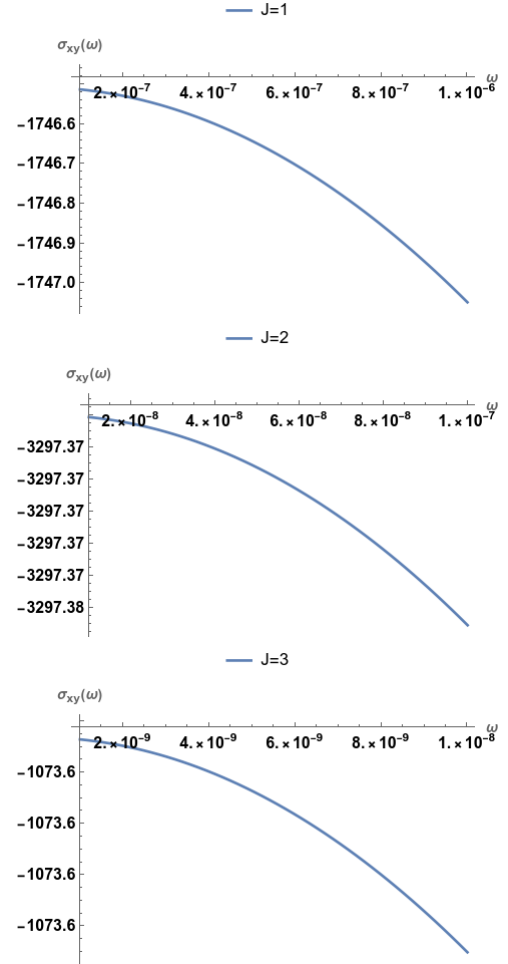


FIG. 3. The frequency dependence of the transverse Hall optical conductivity at  $B = 3$ . The other parameters are taken as  $v_F = 0.005$ ,  $\mu = 0.4$ ,  $\alpha_2 = 3.9 \times 10^{-5}$  and  $\alpha_3 = 2.298 \times 10^{-6}$

- [18] T. Nag and S. Nandy, Magneto-transport phenomena of type-i multi-weyl semimetals in co-planar setups, *Journal of Physics: Condensed Matter* **33**, 075504 (2020).
- [19] A. Menon and B. Basu, Anomalous hall transport in tilted multi-weyl semimetals, *Journal of Physics: Condensed Matter* **33**, 045602 (2020).
- [20] A. Gupta, Novel electric field effects on landau levels in multi-weyl semimetals, *Physics Letters A* **383**, 2339 (2019).
- [21] A. Gupta, Floquet dynamics in multi-weyl semimetals, *arXiv preprint arXiv:1703.07271* (2017).
- [22] A. Gupta, Kerr effects in tilted multi-weyl semimetals, *arXiv preprint arXiv:2209.07506* (2022).
- [23] A. Zyuzin and A. Burkov, Topological response in weyl semimetals and the chiral anomaly, *Physical Review B—Condensed Matter and Materials Physics* **86**, 115133 (2012).
- [24] R. Dantas, F. Peña-Benitez, B. Roy, and P. Surówka, Magnetotransport in multi-weyl semimetals: A kinetic theory approach, *Journal of High Energy Physics* **2018**, 1 (2018).

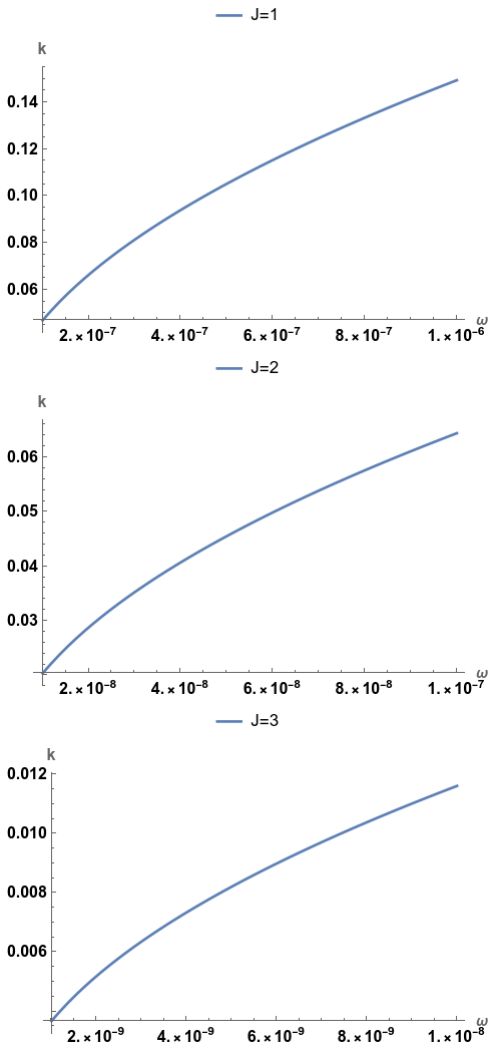


FIG. 4. The  $\omega$  vs.  $k$  dispersion for multi-WSMs at  $B = 3$ . The other parameters are taken as  $v_F = 0.005$ ,  $\mu = 0.4$ ,  $\alpha_2 = 3.9 \times 10^{-5}$  and  $\alpha_3 = 2.298 \times 10^{-6}$ ,  $\epsilon_b = 5$ ,  $b_z = .01\pi/3.5$ ,  $b_0 = 0$  and fine-structure constant  $\alpha = 1/137$

- [25] S. Nandy, C. Zeng, and S. Tewari, Chiral anomaly induced nonlinear hall effect in semimetals with multiple weyl points, *Physical Review B* **104**, 205124 (2021).
- [26] L. Medel, R. Ghosh, A. Martín-Ruiz, and I. Mandal, Electric, thermal, and thermoelectric magnetoconductivity for weyl/multi-weyl semimetals in planar hall set-ups induced by the combined effects of topology and strain, *Scientific Reports* **14**, 21390 (2024).
- [27] D. Xiao, M.-C. Chang, and Q. Niu, Berry phase effects on electronic properties, *Reviews of modern physics* **82**, 1959 (2010).
- [28] Y. Gao, Z.-Q. Zhang, H. Jiang, and K.-H. Ding, Suppression of magneto-optical transport in tilted weyl semimetals by orbital magnetic moment, *Physical Review B* **105**, 165307 (2022).